Electronic Journal of Biotechnology 60 (2022) 58–69

Contents lists available at ScienceDirect

Electronic Journal of Biotechnology

journal homepage: www.elsevier.com/locate/ejbt

Research Article

Bioinformatic approach for the identification of plant species that accumulate palmitoleic acid

Gabriel Salazar Robles [a], Luis Ricardo Hernández [b], Yagul Pedraza Pérez [a], Zaida Nelly Juárez [a], Maricela Rodríguez Acosta [c], Beatriz Pérez Armendáriz [a], Elizabeth Bautista Rodríguez [a], Elie Girgis El Kassis [a,*]

[a] Decanato de Ciencias Biológicas, Universidad Popular Autónoma del Estado de Puebla, Av. 21 Sur 1103, col. Barrio de Santiago, CP 72410 Puebla, Pue., Mexico
[b] Departamento de Ciencias Químico-Biológicas, Universidad de las Américas Puebla, CP 72810 San Andrés Cholula, Pue., Mexico
[c] Herbario y Jardín Botánico Universitario, Benemérita Universidad Autónoma de Puebla Ciudad Universitaria, Av. San Claudio s/n, col. San Manuel, CP 72570 Puebla, Pue., Mexico

GRAPHICAL ABSTRACT

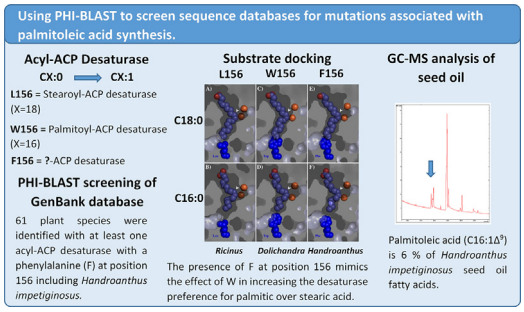

ARTICLE INFO

Article history:
Received 24 April 2022
Accepted 29 September 2022
Available online 6 October 2022

Keywords:
Accumulation
Acyl-ACP desaturase
Bioinformatic approach
Docking modeling
Fatty acid
Handroanthus impetiginosus
Palmitoleic acid
PHI-BLAST
Plants
Seed oil

ABSTRACT

Background: Palmitoleic acid is a fatty acid that possesses nutritional, health, and industrial applications. However, it accumulates in the seed oil of few plant species that often lack agronomic value. A bioinformatics approach was developed as a complementary tool to effort- and time-consuming traditional methods to identify palmitoleic acid-accumulating plant species. The approach involved identifying acyl-ACP desaturases with a sequence variation linked to a switch in the substrate preference from stearic to palmitic acid.

Results: A PHI-BLAST analysis identified *Handroanthus impetiginosus* as a candidate species with two acyl-ACP desaturases with the desired sequence variation. A substrate docking analysis showed that the presence of phenylalanine at the bottom of the active site plays a similar structural role to that of tryptophan present in the same position in the divergent desaturase of the palmitoleic acid accumulator *Dolichandra unguis-cati*. The analysis of the genome of *H. impetiginosus* allowed the identification of four putative ferredoxins, three of which are heterotrophic type and have been linked to an increase in the activity of unusual acyl-ACP desaturases. RT-PCR results showed that both studied *H. impetiginosus* desaturases are expressed in the pod but not in the seeds, while all 4 ferredoxins are expressed in both tissues. GC–MS analysis confirmed the presence of palmitoleic acid in seed oil.

Conclusions: These results suggest that the proposed bioinformatic approach can be a valuable compliment to traditional methods for the identification of plant species that accumulate palmitoleic acid. However, further improvements are needed, such as predicting seed expression of desaturases.

Peer review under responsibility of Pontificia Universidad Católica de Valparaíso.

* Corresponding author.
E-mail address: eliegirgis.elkassis@upaep.mx (E.G. El Kassis).

https://doi.org/10.1016/j.ejbt.2022.09.008

How to cite: Salazar Robles G, Hernández LR, Pedraza Pérez Y, et al. Bioinformatic approach for the identification of plant species that accumulate palmitoleic acid. Electron J Biotechnol 2022;60. https://doi.org/10.1016/j.ejbt.2022.09.008.

1. Introduction

Palmitoleic acid (C16:1Δ^9) is a 16-carbon monounsaturated unusual fatty acid that has several applications in the areas of human nutrition and health, as well as in the industry as a precursor for valuable chemicals and biodiesel production [1]. Pulp oil from sea buckthorn (*Hippophae rhamnoides*), which is enriched in this unusual fatty acid (up to 43%; [2], is used for skin care and the treatment of pathological problems of the gastrointestinal tract mucous membranes [3]. Palmitoleic acid itself is used to reduce inflammation and to prevent diabetes and cardiovascular diseases [4]. It is also a common ingredient in skin care products, since this fatty acid has wound healing, antibacterial, antioxidant, antiaging, and skin lightening properties [1,4].

Palmitoleic acid has received considered interest for its potential applications in the industry. Oils enriched with this fatty acid are considered as a sustainable feedstock for producing 1-octene, which is a raw material for the production of low-density polyethylene, plasticizers, and lubricants [1]. Palmitoleic acid is also considered as a promising feedstock for biodiesel production since it has the potential to greatly improve its physicochemical properties [5,6,7].

However, palmitoleic acid is an unusual fatty acid that few plant species accumulate in significant amounts in their seed or pulp oil [1,7]. These species have often poor agronomic value and/or accumulate small amounts of oil, making them unsuitable for commercial purposes. Some of the plant species that are known to accumulate palmitoleic acid in their oil include *Dolichandra unguis-cati* (∼64%) [1], *Decaisnea insignis* (∼60%) [8], *Tecoma stans* (∼44%) [9], *H. rhamnoides* (∼43%) [2], *Telopea truncata* (∼45%), *Orites diversifolia* (∼41%), *Hicksbeachia pinnatifolia* (∼41%), *Orites revoluta* (∼38%) [1], and *Macadamia integrifolia* (∼24%) [10].

Stearoyl-ACP desaturases (SAD) are soluble enzymes that use their di-iron centers to catalyze the introduction of a double bond between carbons 9 and 10 of stearoyl-ACP to form oleoyl-ACP [11]. Stearoyl-ACP desaturases present a pocket-shaped active site that neatly fits along the entire length of the 18-carbon fatty acid, with the di-iron center positioned near carbons 9 and 10 [11,12,13]. Stearoyl-ACP desaturases present three residues at the bottom of the active site that are important in defining its substrate: 151L, 214 T, and 221G (numbered according to the sequence of *R. communis* stearoyl-ACP desaturase, PDB: P22337). When the enzyme has a bulkier amino acid, such as phenylalanine (F) or tryptophan (W) at one of these three positions at the bottom of the active site, it reduces its size, and the enzyme substrate preference switches from stearic acid to the shorter-chain palmitic acid, leading to the synthesis of palmitoleic acid [12,13,14]. The acyl-ACP desaturase of *D. unguis-cati*, with a tryptophan (W) at position 151, is a typical example. Five other residues play a secondary role in determining substrate specificity of this enzyme: 147M, 148L, 150T, 212P, and 222F [12,13,14,15,16].

Other factors play an important role in the accumulation of unusual fatty acids in seed oil. An acyl-ACP thioesterase with high affinity for C16:1 substrate has been isolated in *Macadamia tetraphylla* and might play an important role in the accumulation of palmitoleic acid in its seed oil [17]. The nature of the ferredoxins that interact with the acyl-ACP desaturase also seems to be another important factor [18]. Ferredoxins are enzymes that are required for the activity of acyl-ACP desaturases, acting as electron donors during the desaturation of a C18:0 to C18:1 [19]. There are 2 types of ferredoxins: heterotrophic and photosynthetic. Schultz et al. [18] demonstrated that heterotrophic ferredoxins isoforms substantially increase the activity of unusual acyl-ACP desaturases.

Traditional methods for identifying fatty acid profiles from oil seed of nonagronomic wild species are often effort and time consuming, in addition to the difficulty of getting sufficient plant material, such as seeds, for oil extraction without damaging an already fragile biodiversity. This considerably slows down the rate at which wild species can be studied and reduces the amount of knowledge available on their fatty acid profiles. Thus, we hypothesized that the development of molecular-based tools to detect the presence of changes associated with palmitoleic acid synthesis might greatly enhance the speed and precision of the process of identifying plant species that can accumulate significant amounts of this unusual fatty acid. DNA can be extracted from any plant tissue, and only small amounts of plant material are required.

To test the validity of this approach, we chose to use bioinformatics tools to identify plant species with desaturases that contain in their sequence residues known to switch their substrate affinity from stearic acid to palmitic acid. We analyzed the GenBank protein database using PHI-BLAST and identified species with desaturases that carry the desired residues. We then proceeded to analyze the gene expression and fatty acid profile of the most promising species to determine whether the presence of these mutations is indeed associated with seed accumulation of palmitoleic acid.

2. Materials and methods

2.1. Identification of candidate species using PHI-BLAST

To determine the PHI-BLAST pattern to be used for the search of candidate species, an initial BLASTp search (https://blast.ncbi.nlm.nih.gov/Blast.cgi) was performed using the *D. unguis-cati* desaturase AAC05293.1, database: nonredundant, and organism: plants (taxid3193). A total of 1542 desaturase sequences were obtained and analyzed using the MEME algorithm of the Meme Suite 5.1.1 (meme-suite.org) for the creation of logos that were used to define the search pattern using PHI-BLAST.

The software BLASTp, using the PHI-BLAST algorithm, was used to search the database for desaturases with the desired residues. The following parameters were used: i) query sequence: AAC05293.1, acyl-ACP desaturase of *D. unguis-cati*, ii) database: nonredundant (nr), iii) organism: plants (taxid 3193), and iv) PHI PATTERN: M-[IVL]-T-E-[ED]-[AS]-[LI]-[PS]-[TS]-Y-[QEHLMN]-[TSA]-[AFGILMQRSTVW]-[AFGILMPV]-[NS]-[GINQRST]-[**FWY**]-[DEL]-[AGNSV]-[AFGILTV]-[AGHKQRSTV]. This pattern represents the residues from position 135 to position 155, using the sequence of the *Ricinus communis* desaturase, P22337.1, as a reference. The bolded letters represent the amino acids in position 151 that corresponds to the L151W mutation in the desaturase of *D. unguis-cati*. The remaining parameters were retained as default.

2.2. Partial sequencing of H. impetiginosus desaturases PIN02096 and PIN00812

Partial sequencing of the genes encoding for the two *H. impetiginosus* desaturases of interest, PIN02096 and PIN00812, was

undertaken to verify that they actually encode for a phenylalanine at positions 148 and 113, respectively, because, in a context, where rare genetic variants are sought, sequencing errors are a profound barrier [20,21]. A PCR product was generated using the specific primers F2096 (5′-GAATTGAGGGAAAGAACC-3′) and R2096 (5′-ATTT GCCCAAGAAGTTGT-3′) for PIN02096, and F3812 (5′-CAGGTGAAG GAATTGAGT-3′) and R2812 (5′-ATATTCACTCGTCCAGAC-3′) for PIN00812. The generated PCR products were sequenced in triplicates using the Sanger capillary sequencing method at the Genomic Services Laboratory of the Langebio-CINVESTAV Institute, Mexico. The obtained sequences were revised and corrected using Chromas (version 2.6.6). The resulting sequences of 113 bp and 204 bp were deposited at GenBank under accession numbers **MT988147** and **MW557597**, respectively.

2.3. Docking of fatty acids in desaturase models

Docking modeling of a C18 and a C16 fatty acid into putative desaturases was made in order to verify the capacity of the active site to harbor fatty acids of different lengths in its interior. Desaturase models of *H. impetiginosus* PIN02096 and PIN00812, and of *D. unguis-cati* AAC05293, were obtained by homology modeling with the User Template function of the online software SWISS MODEL (https://swissmodel.expasy.org), using as template the *R. communis* desaturase protein data bank file 1AFR, all with default settings [22,23,24,25]. The C18 and C16 fatty acids were drawn and geometrically optimized with Avogadro 1.2.0 [26], https://avogadro.cc/). Docking was performed with the AutoDock Vina (ver 1.1.2) function of UCSF Chimera (alpha version 1.15, build 42146), using default settings [27]. The PDB files obtained were visualized with the PyMOL Molecular Graphics System (ver 1.7.x, https://pymol.org/2/).

2.4. Multiple sequence alignment

The alignment of sequences was performed using the Clustal Omega software of EMBL-EBI (https://www.ebi.ac.uk/Tools/msa/clustalo/ [28]. The sequences of acyl-ACP desaturases of the following plant species were aligned: *D. unguis-cati* AAC05293.1, *H. impetiginosus* PIN02096.1 and PIN00812.1, *R. communis* P22337.1, and *Arabidopsis thaliana* NP_186910.2. The alignment was performed using the default parameters and visualized using the BOXSHADE 3.21 tool from Expasy.

2.5. Phylogenetic tree construction

The phylogenetic analysis of the *H. impetiginosus* acyl-ACP desaturases was performed using the software MEGA 10.0.5 according to Chi et al. [29]. They were compared to *A. thaliana* sequences belonging to the 5 groups of desaturases: delta 15 desaturases (AT2G29980; AT5G05580), delta 12 desaturases (AT3G12120; AT4G30950), delta 7/9 desaturases (AT2G46210; AT3G61580; AT4G04930), front-end desaturases (AT3G15850; AT1G06080; AT2G31360), and stearoyl-ACP desaturases (AT3G02630; AT3G02620; AT3G02610; AT2G43710; AT1G43800; AT5G16240; AT5G16230). The phylogenetic tree was built using the Neighbor-Joining Method, with a Bootstrap analysis using 1000 replicates and a Poisson model as a substitution model. Other parameters were retained as default.

Ferredoxin-like encoding sequences from *H. impetiginosus* were searched using the BLAST software. The *A. thaliana* ferredoxin-encoding gene with accession number NP_176291.1 was used as a query and was compared to the nonredundant protein sequences (nr) database, limiting the results for the organism *Handroanthus impetiginosus* (taxid: 429701). The phylogenetic analysis of the *H. impetiginosus* ferredoxins was performed using the software MEGA 10.0.5 following the tree published by Venegas-Calerón et al. [30] using the same parameters described above. The following sequences were used: *Triticum aestivum* (Ta2, gi462081), *Zea mays* (Zm1, gi119928; Zm2, gi119961), *A. thaliana* (AtFD1, gi15220256; AtFD2, gi15219837; AtFD3, gi15225888), *Helianthus annuus* (HaFd1, gi37779195; HaFd2, gi68137465), *Impatiens balsamina* (Ib1, gi13182955), *Mesembryanthemum crystallinum* (Mc1, gi3023743), *Pisum sativum* (Ps1, gi119931), *Silene latifolia* (Sil1, gi120026), *Solanum lycopersicum* (Sol1, gi3023752), *Spinacia oleracea* (So1, gi119937), and *H. impetiginosus* (PIN14867.1, PIN25422.1, PIN00097.1, and PIN26937.1).

2.6. Sample collection of Handroanthus impetiginosus

Developing and mature seeds and pod samples were collected from a *H. impetiginosus* tree located in Xicotlán, Puebla, Mexico (N18°03′29.43′′, W98°31′36.22′′) toward the end of February. Samples were stored at −80°C.

2.7. Soxhlet extraction of seed oil

Seed and pericarp samples were lyophilized under vacuum with a collector temperature of −50°C for 24 h, using a FreeZone 2.5 L freeze drier (Labconco). Oil was extracted from samples (20 g each) using a 250 mL Soxhlet apparatus (SEV, catalogue number 178-3). HPLC Grade heptane (Karal, catalogue number 9014) (150 mL) was used as the extraction solvent and was recirculated for 6 h under heating at 80°C. Heptane was evaporated under vacuum at 70°C and 50 rpm using a Hahnvapor HS-2001NS rotary evaporator (Hahn Shin Scientific). The residual solvent was evaporated using high-purity nitrogen gas flow. Oil samples were stored at −20°C prior to transesterification.

2.8. Determination of fatty acid profile using GC–MS

For the chromatographic analysis of fatty acid methyl esters (FAMEs), a CP3800 gas chromatograph (Varian) coupled to a Varian-4000 mass spectrometer (Varian) and a VF-5 ms (catalogue number CP8944), 30 m long, 0.25 mm in diameter, and 0.25 μm thick capillary column were used. Helium was used as a carrier gas with a flow of 1.1 mL/min. The temperature ramp in the column was started at 60°C for 2 min, increased to 280°C at a rate of 10°C/min, maintaining the temperature for 6 min. A volume of 0.1 mL of the sample was injected into the column in the splitless mode, using a Combi Pal autosampler (Pal System). The injector temperature was set at 250°C. The mass spectrometer was operated at 70 eV, and the mass range was 40 to 425 uma. The identification of compounds was performed using the NIST Mass Spectral Search program, by comparing their fragmentation profile to the NIST/EPA/NIH mass spectral library (Version 2.0 d, Build Dec 2, 2005).

2.9. Determination of gene expression using Reverse-Transcription PCR

RNA was extracted from pods, developing, and mature seeds using the RNeasy PowerPlant Kit (Qiagen, Valencia, CA, USA) according to the manufacturer's instructions. RNA samples were stored at −80°C until further processing. Reverse-transcription reactions were performed using the QuantiTect Reverse Transcription Kit (Qiagen, Valencia, CA, USA) according to the manufacturer's instructions, with 120 ng of total RNA were used for each reaction. The RT Primer Mix provided with the kit was used for each reaction. Leaves were also considered for RNA extraction; however, persistent presence of PCR inhibitors in the samples did not permit obtaining satisfactory gene expression results for

leaves. The primers used for cDNA amplification are shown in Table 1.

2.10. Transesterification of fatty acids

Fatty acid transesterification was performed using the method described by Ichihara and Fukubayashi [31] with modifications. Briefly, the oil sample was dissolved with 0.2 mL of toluene in a 4 ml glass tube. Then, 1.5 mL of methanol and 0.3 mL of HCl/methanol 8% (v/v) solution were added. The reaction was mixed using a vortex and incubated at 80°C for 1 h in a water bath. Then, the reaction was allowed to cool down to room temperature, and fatty acids were extracted twice using 2 mL of heptane. The solvent was evaporated using high purity nitrogen gas flow. FAMEs were then dissolved in 200 μL of heptane and were stored at −20°C prior to GC–MS analysis.

3. Results

3.1. Identification of acyl-ACP desaturases with W, F, or Y in position 151

To identify acyl-ACP desaturases that present a bulky amino acid at the bottom of their active site, the GenBank database was searched using PHI-Blast. The search was performed using a pattern that consisted of 21 amino acids (positions 135 to 155) around the L151 residue, representing the consensus local sequence of 1542 acyl-ACP desaturases, except for position 151, where L was replaced with W, F, or Y. The search resulted in the identification of 168 sequences of which 154 sequences (belonging to 61 species) presented an F at position 151 (Table 2), 16 sequences (belonging to 5 species) presented a Y at that same position (Table 3), and 6 sequences (belonging to 4 species) presented a W (Table 4). Of all the identified species, *H. impetiginosus,* a tree belonging to the Bignoniaceae family (Table 2), was chosen for further study.

3.2. Phylogenetic analysis of H. impetiginosus desaturases

H. impetiginosus possess 15 acyl-ACP desaturases (Fig. S1), two of which present a phenylalanine (F) at position 151, PIN02096.1 and PIN00812.1 (Table 2). The presence of an F at position 151 was verified by partial sequencing of both desaturases. Fatty acid desaturases usually belong to five groups: stearoyl-ACP desaturases, front-end desaturases, delta 7/9 desaturases, delta 12 desaturases, and delta 15 desaturases [29]. To verify to which desaturase group PIN02096 and PIN00812 belong, they were compared to *A. thaliana* fatty acid desaturases belonging to the 5 desaturases groups (Fig. 1). The phylogenetic analysis showed that PIN02096.1 and PIN00812.1 belong to the stearoyl-ACP desaturase group.

3.3. C16 and C18 fatty acid docking modeling for the acyl-ACP desaturases

The docking modeling was performed in order to evaluate the capacity of each of the desaturases to harbor a C18 or a C16 fatty acid in their active site. The results are shown in Fig. 2. The docking simulation of the *R. communis* desaturase P22337 (Fig. 2A and 2B) showed that its active site can accommodate a C18 fatty acid, with carbons 9 and 10 aligned with the di-iron catalytic center (Fig. 2A). A similar result is obtained when the docking of a C16 fatty acid is simulated (Fig. 2B). The docking simulation of the *D. unguis-cati* desaturase AAC05293.1 (Fig. 2C and 2D) showed that its active site can accommodate a C16 fatty acid, with carbons 9 and 10 aligned with the di-iron catalytic center (Fig. 2D). However, a C18 fatty acid does not fit well in the active site of this desaturase due to the presence of the bulky tryptophan at the bottom of the active site (Fig. 2C). The docking simulation of the *H. impetiginosus* desaturases PIN02096.1 (Fig. 2E and 2F) and PIN00812.1 (Fig. 2G and 2H) showed similar results to those obtained with the desaturase of *D. unguis-cati*. A C16 fatty acid fits comfortably in their active site, with carbons 9 and 10 aligned with the di-iron catalytic center (Fig. 2F and 2H), while a C18 fatty acid does not fit well due to the presence of the bulky phenylalanine at the bottom of the active site (Fig. 2E and 2G).

3.4. Sequence alignment of acyl-ACP desaturases

To verify whether any of the two *H. impetiginosus* acyl-ACP desaturases with a phenylalanine at the bottom of their active site present any additional residue at locations that have been previously linked to an increased affinity for palmitic acid as a substrate, their sequences were compared to that of *A. thaliana* and *D. unguis-cati* acyl-ACP desaturases that have been shown to be implicated in the synthesis of palmitoleic acid (Fig. 3) [13,14]. *R. communis* and *A. thaliana* desaturases with affinity for stearic acid as a substrate were also included in the multiple sequence alignment. The 8 amino acid positions that have been proposed to be implicated in altering the specificity of the desaturase for stearic acid as a substrate [12,13,32] are indicated with a star in Fig. 3. *H. impetiginosus* desaturase PIN02096 presents variations at 5 of these 8 positions: M147W, L148I, T150S, L151F, and P212L. *H. impetiginosus* desaturase PIN00812 presents variations at 3 of these 8 positions: M147L, L151F, and T214I. These results suggest that PIN02096 and PIN00812 are potential Δ^9 palmitoyl-ACP desaturases.

Table 1
Primers used for cDNA amplification.

Name	Sequence (5′-3′)	Amplicon size (pb)	Target gene	Gene function
Fr097F	CGGATGGTTCCGAGTGTGAG	145	PIN00097	Heterotrophic ferredoxin
Fr097R	TCAACAGTACCCGATGCCAA			
Fr867F	AGCCCCGTCAATCAAATCCAA	157	PIN14867	Heterotrophic ferredoxin
Fr867R	CTCCCCTTCTGGACCGATCA			
Fr422F	CACCCGAACTACAACTGCCT	173	PIN25422	Heterotrophic ferredoxin
Fr422R	CAGGGGCCTCAAACTCACAT			
Fr937F	TCGGTCTCAAAACCACAGGC	109	PIN26937	Photosynthetic ferredoxin
Fr937R	GTGTCATGTGGGCACTCGAT			
F2096	GAA TTG AGG GAA AGA ACC	159	PIN02096	Acyl-ACP desaturase
R2096	ATT TGC CCA AGA AGT TGT			
F3821	CAG GTG AAG GAA TTG AGT	251	PIN00812	Acyl-ACP desaturase
R2812	ATA TTC ACT CGT CCA GAC			
HIEF1αF	ATG CCC CCG GAC ATC GTG ACT TTA T	1350	HIEF1αF	Elongation factor (control gene)
HIEF1αR	TTG GCC GCT TCC TTT GCA GGA TCA			

Table 2
Plant species identified using the PHI-BLAST search that present a phenylalanine at residue 151 of the acyl-ACP desaturase. The maximum percentage of palmitoleic acid is shown when available according to the Plant FAdb database (https://plantfadb.org/). NA: Not available.

Family	Species	Accession number	C16:1Δ^9 (%)
Amaranthaceae	*Beta vulgaris* subsp. *Vulgaris*	XP_010672435.1, XP_019104189.1	NA
	Chenopodium quinoa	XP_021774822.1, XP_021774823.1	0.1
	Spinacia oleracea	XP_021845524.1, KNA20751.1	0.3
Araceae	*Colocasia esculenta*	MQL73192.1	NA
	Spirodela intermedia	CAA7406462.1	NA
Arecaceae	*Elaeis guineensis*	XP_010933036.1	0
	Phoenix dactylifera	XP_008776791.1	0
	Cocos nucifera	EHA8588056.1, EHA8588529.1	0
Asparagaceae	*Asparagus officinalis*	XP_020263717.1	0.1
Asteraceae	*Mikania micrantha*	KAD3067296.1	NA
Bignoniaceae	***Handroanthus impetiginosus***	**PIN02096.1, PIN00812.1**	**NA**
Celastraceae	*Tripterygium wilfordii*	KAF5742783.1	3.7
Ditrichaceae	*Ceratodon purpureus*	KAG0589170.1, KAG0628101.1	NA
Fabaceae	*Senna tora*	KAF7829757.1	0.58
Funariaceae	*Physcomitrella patens*	XP_024373918.1, XP_024391803.1, XP_024392006.1	NA
Lauraceae	*Cinnamomum micranthum*	RWR74611.1	NA
Marchantiaceae	*Marchantia paleacea*	KAG6549030.1	NA
	Marchantia polymorpha	PTQ43616.1	NA
	Marchantia polymorpha subsp. *Ruderalis*	OAE25297.1	NA
Musaceae	*Ensete ventricosum*	RRT85166.1, RWW12509.1, RZS27645.1, RWW75243.1	NA
Orchidaceae	*Apostasia shenzhenica*	PKA52413.1	NA
	Ophrys garganica	AFD28971.1, AFD28970.1, AFD28969.1, AFD28967.1	NA
	Ophrys sphegodes	AFQ59993.1, AIY68656.1, AFD28975.1, AFD28974.1, AFD28972.1, AFD28976.1	NA
	Ophrys × *arachnitiformis* subsp. *archipelagi*	AIY68657.1, AKO71444.1, AFQ59991.1, AFQ59992.1, AFD28966.1, AFD28968.1, AFF19383.1, AFD28982.1, AFD28977.1, AFD28979.1, AFF19390.1, AFD28980.1, AFD28981.1, AFF19393.1, AFF19394.1, AFF19385.1, AFF19387.1, AFF19389.1, AFF19384.1, AFF19386.1, AFF19392.1, AFD28978.1	NA
	Phalaenopsis equestris	XP_020573435.1	NA
	Vanilla planifolia	KAG0500705.1, KAG0496230.1	NA
Orobanchaceae	*Phtheirospermum japonicum*	GFQ06064.1, GFP95611.1	NA
Phoeniceae	*Phoenix dactylifera*	XP_038982871.1, XP_038982870.1	0.11
Phrymaceae	*Erythranthe guttata*	XP_012839061.1	NA
Poaceae	*Aegilops tauschii subsp. Tauschii*	XP_020163833.1, XP_020163590.1, XP_020173898.1	NA
	Digitaria exilis	CAB3480308.1, CAB3502374.1, KAF8662556.1, KAF8774992.1	NA
	Eragrostis curvula	TVU03244.1, TVU02099.1, TVU02100.1	NA
	Miscanthus lutarioriparius	CAD6265946.1, CAD6246996.1	NA
	Oryza brachyantha	XP_006659916.1, XP_006659916.2	NA
	Oryza meyeriana var. granulata	KAF0899449.1, KAF0899446.1	NA
	Panicum hallii	XP_025821525.1, XP_025821524.1	NA
	Panicum hallii var. *Hallii*	PUZ50477.1	NA
	Triticum turgidum subsp. *Durum*	VAH41460.1, VAH25667.1, VAH25666.1, VAH41461.1, VAH25664.1, VAH25665.1, VAH41467.1	NA
	Hordeum vulgare	KAE8772682.1, KAE8801960.1	0.14
	Oryza sativa	KAB8093503.1	0
	Oryza sativa Japonica Group	XP_015649776.1, EAZ41833.1, XP_025883319.1, KAF2941233.1, AAR87311.1, EAZ28531.1	0
	Panicum miliaceum	RLN03816.1	0
	Panicum virgatum	XP_039855810.1, XP_039815032.1, KAG2577334.1	NA
	Sorghum bicolor	XP_002444003.2, KAG0522868.1	3.6
	Triticum aestivum	SPT16023.1, SPT16024.1, SPT16028.1, KAF7006344.1, KAF7013653.1, KAF6999037.1, KAF7006348.1, KAF7006349.1	0.1
	Triticum dicoccoides	XP_037475554.1, XP_037483247.1, XP_037483246.1	NA
	Zea mays	NP_001168371.1, XP_008662134.1, PWZ43910.1	0.1
Selaginellaceae	*Selaginella moellendorffii*	XP_002967979.2, EFJ31326.1, XP_024524536.1, EFJ34273.1	NA
Solanaceae	*Capsicum baccatum*	PHT45335.1	NA
	Capsicum chinense	PHU14529.1	NA
	Solanum chilense	TMW82197.1, TMW88013.1	NA
	Solanum commersonii	KAG5601018.1, KAG5601023.1, KAG5600429.1	NA
	Solanum pennellii	XP_015078034.1	NA
	Capsicum annuum	XP_016575233.1, KAF3627191.1	1.7
	Nicotiana sylvestris	XP_009767980.1	6.3
	Nicotiana tabacum	XP_016460159.1	3.2
	Solanum lycopersicum	XP_004242060.1, XP_004242061.1	0.5
	Solanum tuberosum	XP_006356733.1, XP_006357932.1	0.1
Theaceae	*Camellia sinensis* var. *Sinensis*	THG17476.1	NA
	Camellia sinensis	XP_028062583.1, XP_028062584.1, KAF5942202.1	0.9
Triticeae	*Triticum aestivum*	KAF7013652.1, KAF7013654.1, KAF6999038.1	0.1

Table 3
Plant species identified using the PHI-BLAST search that present a tyrosine at residue 151 of the acyl-ACP desaturase. The maximum percentage of palmitoleic acid is shown if available. NA: Not available.

Family	Species	Accession number	C16:1Δ^9 (%)
Asteraceae	*Cynara cardunculus* var. *Scolymus*	XP_024966035.1, XP_024966743.1	0.3
Nyssaceae	*Nyssa sinensis*	KAA8532143.1	1.4
Theaceae	*Camellia oleifera*	AZL94135.1	0.35
	Camellia sinensis	XP_028110737.1, XP_028062581.1, XP_028062580.1, XP_028062582.1, XP_028065038.1, KAF5942204.1, KAF5942200.1	0.9
Zingiberaceae	*Zingiber officinale*	KAG6512249.1, KAG6509420.1, KAG6515603.1, KAG6509419.1, KAA8532143.1	NA

Table 4
Plant species identified using the PHI-BLAST search that present a tryptophan at residue 151 of the acyl-ACP desaturase. The maximum percentage of palmitoleic acid is shown if available. NA: Not available.

Family	Species	Accession number	C16:1Δ^9 (%)
Bignoniaceae	*Dolichandra unguis-cati*	AAC05293.1	64
Juglandaceae	*Carya illinoinensis*	KAG6671684.1, KAG2663215.1, KAG6624316.1	0.1
Orobanchaceae	*Striga asiatica*	GER27903.1	NA
Solanaceae	*Solanum tuberosum*	XP_006356735.1	0.1

3.5. Phylogenetic analysis of H. impetiginosus ferredoxins

To identify the *H. impetiginosus* heterotrophic ferredoxins, which would increase its capacity to synthesize unusual fatty acids, a BLAST search was performed using the sunflower photosynthetic (HaFd1; AAO42615.1) and heterotrophic (HaFd2; AAY85661.1) ferredoxins [30]. Four ferredoxin-like genes were identified encoding for the proteins PIN26937.1, PIN14867.1, PIN25422.1, and PIN00097.1. A phylogenetic analysis was performed to determine to which group the four *H. impetiginosus* ferredoxins belong to through their comparison with other photosynthetic and heterotrophic ferredoxins. The results are shown in Fig. 4. Three out of four *H. impetiginosus* ferredoxins (PIN14867.1, PIN25422.1, and PIN00097.1) clustered with the heterotrophic group, while only one ferredoxin (PIN26937.1) clustered with the photosynthetic group.

3.6. Gene expression analysis of desaturases and ferredoxins

Reverse transcription PCR was used to determine the gene expression of two putative acyl-ACP desaturases and four putative ferredoxins in pods, developing, and mature seeds of *H. impetiginosus*. PIN02096 and PIN00812 acyl-ACP desaturases were expressed in pods but not in developing or mature seeds (Fig. 5). On the other hand, the heterotrophic ferredoxins PIN14867, PIN25422, and PIN00097 were expressed in all the tested tissues (Fig. 5). However, PIN25422 showed very low expression levels in the pod. The photosynthetic ferredoxin PIN26937 was expressed in pods and developing seeds but not in mature seeds (Fig. 5).

3.7. Fatty acid profile

To determine the presence of palmitoleic acid in the seed oil of *H. impetiginosus*, its FAMEs were analyzed using GC–MS. The seed oil content was 18.6 ± 3.6% (w/w) of oil per gram of seeds. The relative abundance of the detected fatty acids is shown in Table 5. The most abundant fatty acid was oleic acid (45.9%), followed by linoleic (22.1%) and palmitic (10.4%) acids. Palmitoleic acid was the fifth most abundant fatty acid with 6%. Monounsaturated fatty acids represented more than half of the total fatty acids with the rest divided evenly between saturated and polyunsaturated fatty acids.

4. Discussion

The PHI-Blast analysis of plant acyl-ACP desaturases revealed that the L151F variation is by far the most abundant in the genomes of the studied plant species (Table 2), with only few sequences presenting the L151W (Table 3) and L151Y variations (Table 4). This is to be expected since the change of only one base is needed to switch the codon that encodes for leucine to the one encoding for phenylalanine. By contrast, the codons that encode for tryptophan and tyrosine would require two bases to be changed.

The results shown in Table 1, Table 2, and Table 3 indicate that the majority of plant species with known SAD sequences in GenBank that have a bulky amino acid at position 151 (F, Y, or W), and have their seed fatty acid profile reported, do not accumulate a high or even significant percentage of palmitoleic acid in their seeds. These results are obviously biased toward species that have both their DNA sequence and seed fatty acid profile available. However, they seem to indicate that possessing a divergent desaturase with a bulky residue might not be enough for the plant species to accumulate palmitoleic acid in their seeds, and that other factors might be involved [1,34].

Of all the plant species that were identified, *H. impetiginosus* (Table 2) caught our attention since it belongs to the bignoniaceae family, the same family the palmitoleic acid accumulator *D. unguis-cati* belongs to. *H. impetiginosus* possesses two putative fatty acid desaturases with a phenylalanine (F) at position 151, PIN02096 and PIN00812. Thus, we expected *H. impetiginosus* to show at least a moderate percentage of palmitoleic acid in its seed oil. Additionally, *H. impetiginosus* is the only member of the bignoniaceae family whose whole genome has been sequenced. It is also an endangered species; hence, its study might help foster its conservation [35].

Phylogenetic analysis of PIN02096 and PIN00812 (Fig. 1) verified that they belong to the stearoyl-ACP desaturases group. This indicates that they are likely soluble enzymes involved in the first desaturation of saturated fatty acids [36]. As the group name indicates, their usual substrate is stearoyl-ACP (C18:0-ACP). However, their substrate preference could shift to palmitoyl-ACP (C16:0-ACP) due to the presence of a bulky amino acid at the bottom of the active site that leads to a reduction in its size. A multiple sequence alignment analysis was performed where sequences of PINI2096 and PIN00812 were compared to that of other desaturases with preference to stearoyl-ACP or palmitoyl-ACP as a substrate (Fig. 3). The results showed that both *H. impetiginosus* desaturases present several residues variations, 5 for PINI2096 and 3 for PIN00812, in positions associated with a shift in the desaturase substrate preference toward palmitoyl-ACP [12,13,32]. This includes the presence, in both desaturases, of the bulky phenylalanine (F) at position 151. Taken together, these results suggest that PIN02096 and PIN00812 could potentially function as palmitoyl- rather than stearoyl-ACP desaturases.

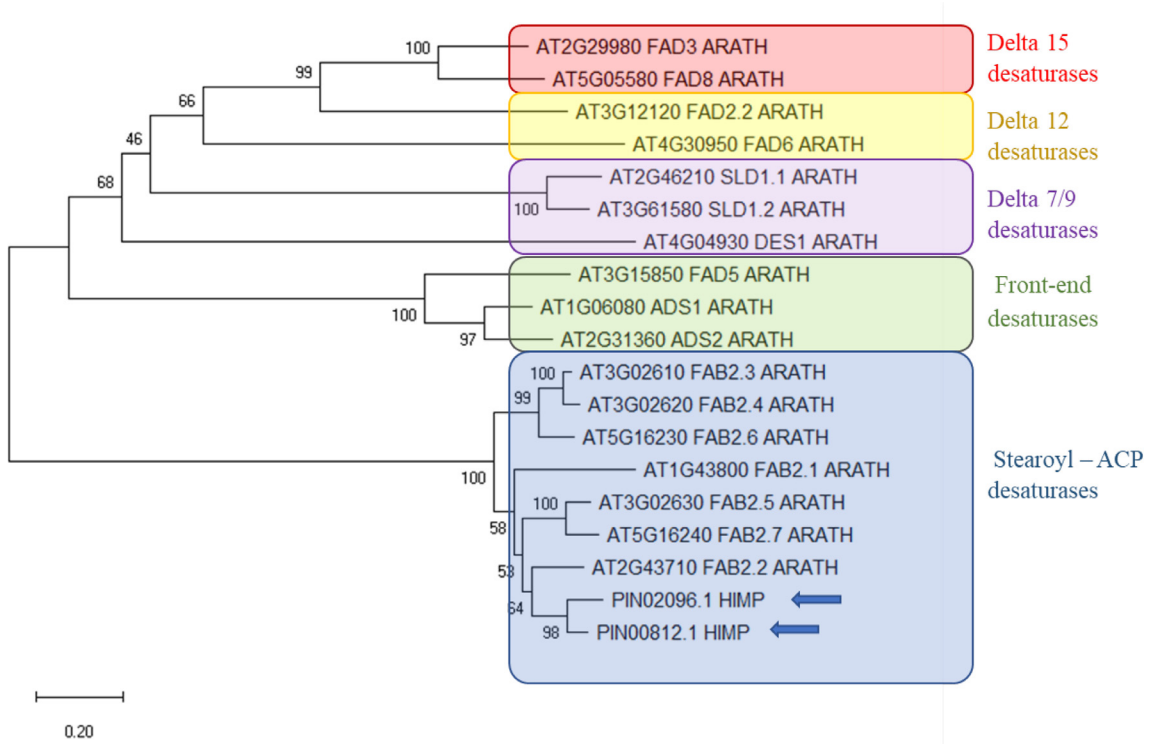

Fig. 1. Phylogenetic analysis of the 5 groups of fatty acid desaturases. Both isoforms of *H. impetiginosus* PIN02096.1 and PIN00812.1 clustered with the *A. thaliana* stearoyl-ACP desaturases. Their position is indicated with an arrow. The evolutionary history was inferred using the Neighbor-Joining Method [33]. The percentage of replicate trees in which the associated taxa clustered together in the bootstrap test (1000 replicates) is shown next to the branches. The evolutionary distances were computed using the Poisson correction method and are in the units of the number of amino acid substitutions per site (Adapted from Chi et al. [29]).

While phenylalanine can be considered as a "bulky" amino acid similarly to tryptophan, it possesses a somewhat smaller in size. To determine whether the presence of phenylalanine at the bottom of the active site provokes similar consequences to that generated by the presence of tryptophan at the same position, we performed a docking modeling of stearic acid and palmitic acid into a 3D model of *R. communis*, *D. unguis-cati,* and *H. impetiginosus* desaturases (Fig. 2). The results showed that the presence of a leucine at the bottom of the active site of the desaturase of *R. communis* causes stearic acid to fit neatly in the active site (Fig. 2A). While palmitic acid seems to fit in the active site of *R. communis* desaturase (Fig. 2B), the affinity of the enzyme for this substrate is very low compared to stearic acid [15]. It is likely that the preferred substrate of the desaturase is a fatty acid that reaches the bottom of the active site. As expected, the presence of the bulky tryptophan at the bottom of the active site of *D. unguis-cati* desaturase caused a reduction of its size. This resulted in the shorter palmitic acid fitting neatly in the active site (Fig. 2C) as compared to the longer stearic acid that seems to be obstructed by the presence of tryptophan (Fig. 2D). These results are in agreement with previously published reports [12,14]. The substrate docking modeling of both *H. impetiginosus* desaturases showed a similar result to that observed with the *D. unguis-cati* desaturase. The presence of phenylalanine at the bottom of the active site led to a reduction of its size and a better fitting of palmitic acid (Fig. 2F and 2H) than stearic acid (Fig. 2E and 2G) as a substrate. It is important to note that in all cases, carbons 9 and 10 of the fatty acid aligned with the di-iron catalytic center (Fig. 2). These results suggest that phenylalanine is likely to play a role similar to that of tryptophan in changing the structure of the desaturasés active site, shifting its substrate preference from stearoyl-ACP to palmitoyl-ACP.

It is important to note that the presence of tryptophan in position 151 seems to be sufficient by itself to switch the desaturase preference from stearic acid to palmitic acid. The sequence of the *D. unguis-cati* desaturase (Fig. 3) does not show the presence of any other variation in sites associated with a preference of the desaturase to palmitic acid. Contrary to tryptophan, the presence of phenylalanine in position 151 does not seem to be sufficient by itself to switch the desaturase preference from stearic acid to palmitic acid. In an experiment, reported by Cahoon and Shanklin [15], where the sequence of *R. communis* stearoyl-ACP desaturase was mutated to replace the leucine in position 151 with a phenylalanine, the preferred substrate of the mutated desaturase was shown to be stearoyl-ACP, even if the affinity of the enzyme for palmitoyl-ACP increased compared to the wild-type desaturase. However, the double mutant L151F/P212I of the same enzyme showed a higher preference for palmitoyl-ACP as a substrate than for stearoyl-ACP [12]. Position 212 is one of the positions associated with a switch of the preference of the desaturase to palmitoyl-ACP as a substrate (Fig. 3). The presence in both *H. impetiginosus* desaturases, PINI2096 and PIN00812, of 5 and 3 variations respectively, in positions associated with the enzyme preference to palmitoyl-ACP, further supports the hypothesis that they may actually function as palmitoyl-ACP desaturases.

This also provides a partial explanation regarding why so many of the plant species that contain stearoyl-ACP desaturases with a phenylalanine in position 151 do not accumulate significant amounts of palmitoleic acid in their seed oil (Table 1). It is possible that the sequences of the stearoyl-ACP desaturases of some of these species do not possess the necessary additional variations of residues in the right positions. However, other factors might also explain the lack of accumulation of palmitoleic acid in the seed oil

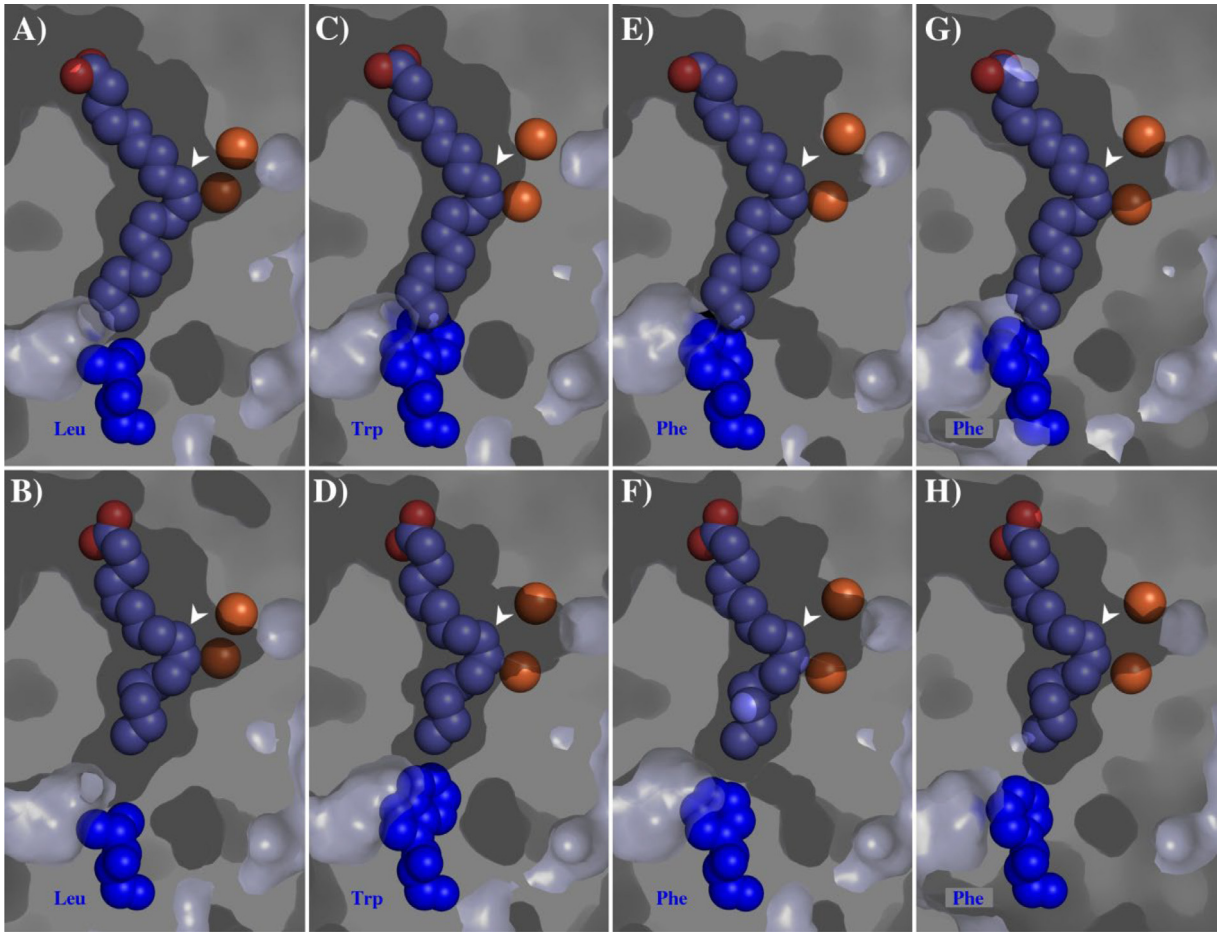

Fig. 2. Docking simulation of C16 and C18 fatty acids in the active site of acyl-ACP desaturases of *R. communis*, *D. unguis-cati*, and *H. impetiginosus*. The image shows the pocket of the active site, with the corresponding fatty acid and the residue at position 151 shown at the bottom (in blue): A) and B) *R. communis* P22337.1 desaturase with a leucine at the bottom of the active site, C) and D) *D. unguis-cati* AAC05392.1 desaturase with a tryptophan at the bottom of the active site, E) and F) *H. impetiginosus* PIN02096.1 desaturase, G) and H) *H. impetiginosus* PIN00812.1 desaturase, both with a phenylalanine at the bottom of the active site. In A), C), E), and G) docking was performed with a C18 fatty acid. In B), D), F), and H) docking was performed with a C16 fatty acid. The di-iron catalytic center is represented by brown spheres. Carbon 9 position is indicated by a white arrow. The models were visualized with PyMOL Molecular Graphics System, Version 1.7.x.

of species that possess acyl-ACP desaturases with variations that favor palmitoyl-ACP as a substrate. It is possible that these divergent acyl-ACP desaturases are simply not expressed in the seeds or are not the dominant desaturases in the seed. In some cases, their expression is limited to a particular tissue of the seed, different from the one where the fatty acids accumulate, as in the case of *A. thaliana* [13]. Another possibility is that the consumption of the synthesized palmitoleic acid as a substrate for subsequent biochemical reactions, which prevent its accumulation in the seed. Palmitoyl-ACP is the substrate for more than four biochemical pathways. The final results depend on the different enzymes affinities and catalytical speeds. The insertion in transgenic plants of genes encoding for palmitoyl-ACP desaturases only led to a modest increase in the accumulation of palmitoleic acid in seed oil [34,37]. Further tweaking of the involved metabolic fluxes was actually necessary to achieve an accumulation of a high percentage of palmitoleic acid in seed oil, providing further evidence that it is a multifactorial process.

Two factors that seem to be important for the accumulation of unusual fatty acids in seeds, is the presence of compatible acyl carrier proteins (ACP) and ferredoxins. Kazaz et al. [38] reported that specific isoforms of ACP are involved in the biosynthesis of various C16:1 isoforms (C16:1Δ^4, Δ^6, Δ^9). It is reasonable to assume that this is the case for palmitoleic acid. However, no information is currently available on the nature of the variations that make an ACP more compatible with the various isoforms of C16:1 fatty acid.

The presence of heterotrophic ferredoxins has been previously linked to a significant increase in the activity of unusual acyl-ACP desaturases [18]. Phylogenetic analysis showed that three of the four ferredoxins are heterotrophic, and only one is photosynthetic (Fig. 4).

Gene expression results (Fig. 5) showed that both desaturases of interest, PIN02096 and PIN00812, are expressed in pods but not in developing or mature seeds. However, the analysis of seed and pod fatty acid profiles show that palmitoleic acid accumulates in the seed (Table 5) but not in the pods (data not shown). These results suggest that it is likely that palmitoleic acid is synthesized in the pods and subsequently transferred to the seeds. Another possibility is that putative palmitoyl-ACP desaturases themselves might be synthesized in the pod and then transferred to the developing seed. It has been reported that one of the pod functions is supplying nutrients, and potentially proteins and enzymes, to the developing seed [39,40]. Putative ferredoxin-encoding gene expression results (Fig. 5) indicate that the three putative heterotrophic ferredoxins in addition to the lone photosynthetic ferredoxin are all expressed in the pods. Thus, they all have the potential to interact with the putative palmitoyl-ACP desaturases PIN02096 and PIN00812. It is thus possible that the heterotrophic forms interact preferentially with PIN02096 and PIN00812 in order to increase their putative

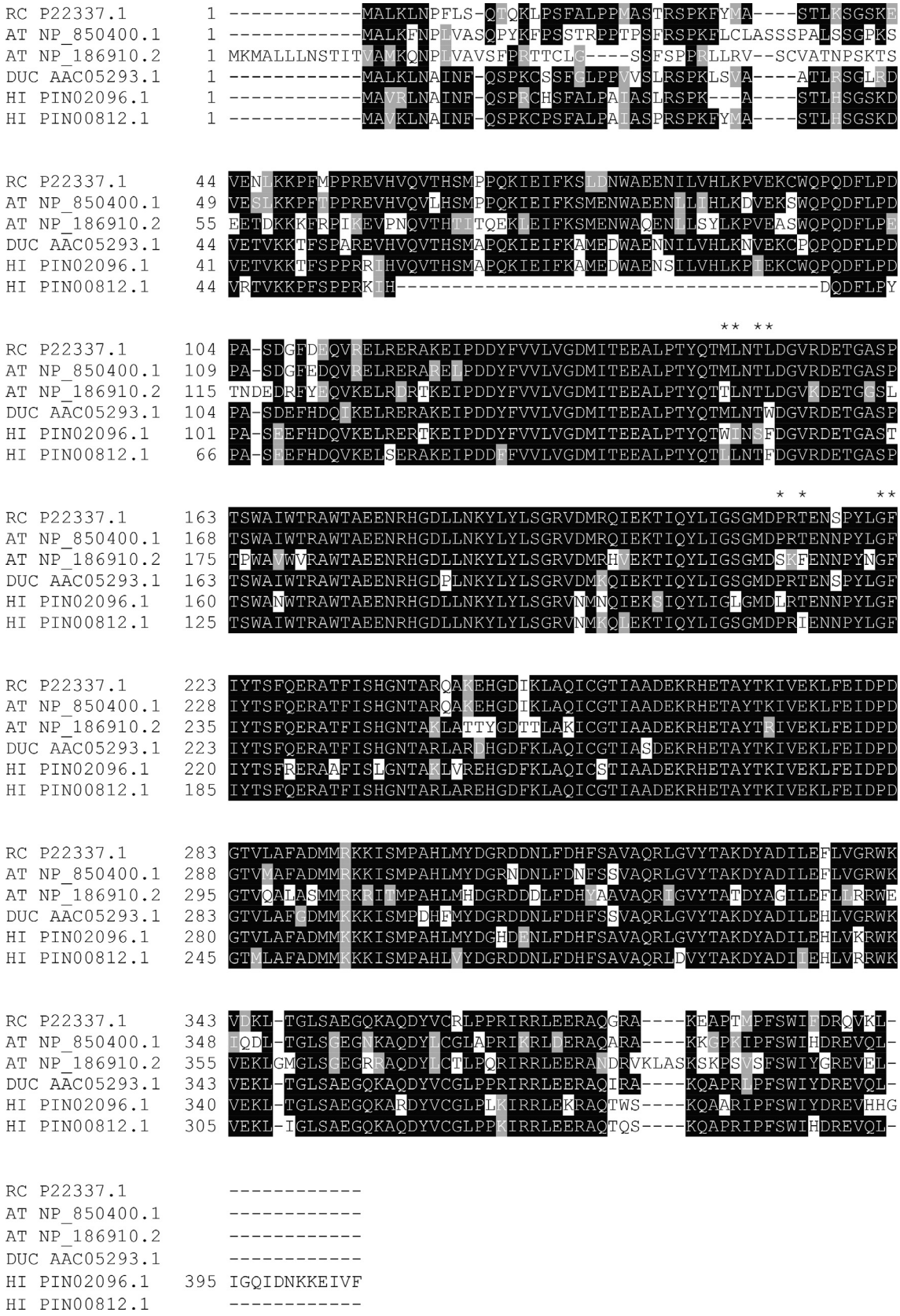

Fig. 3. Comparison of the sequences of putative *D. unguis-cati* Δ^9 palmitoyl-ACP desaturases to that of other palmitoyl- and stearoyl-ACP desaturases. *R. communis* (RC) desaturase P22337 and *A. thaliana* (AT) desaturase NP_850400 were used as representatives of stearoyl-ACP desaturases. *A. thaliana* desaturase NP_186910 and *D. unguis-cati* (DUC) desaturase AAC05293 were used as representatives of palmitoyl-ACP desaturases. Amino acid residue positions that are important for altering substrate specificity from stearic acid to palmitic acid are marked with an asterisk.

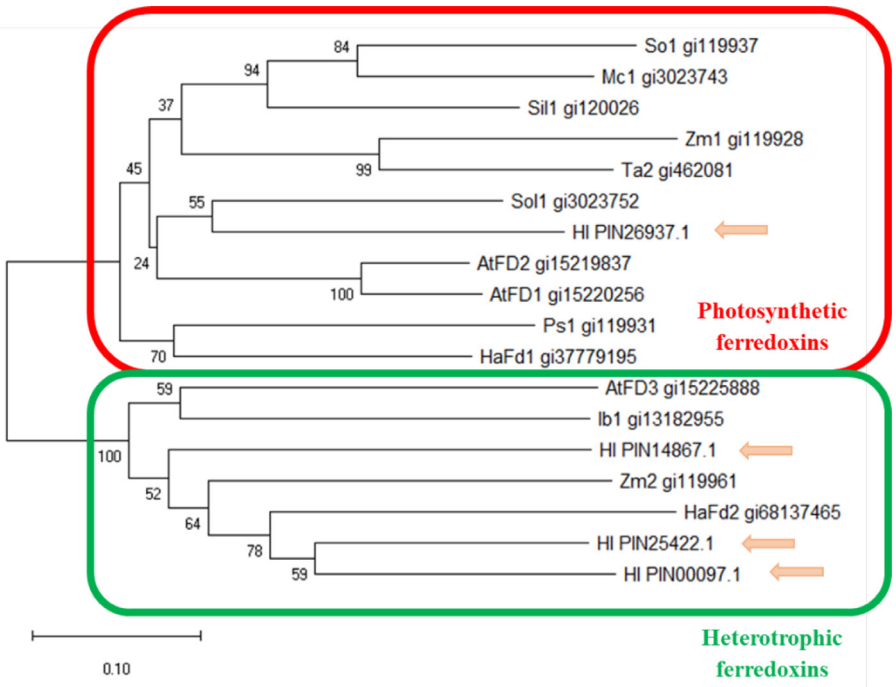

Fig. 4. Phylogenetic analysis of heterotrophic and photosynthetic ferredoxins. *H. impetiginosus* ferredoxins PIN14867.1, PIN25422.1, and PIN00097.1 clustered with the heterotrophic group. *H. impetiginosus* ferredoxin PIN26937.1 clustered with the photosynthetic group. Their position is indicated with an arrow. The evolutionary history was inferred using the Neighbor-Joining Method [33]. The percentage of replicate trees in which the associated taxa clustered together in the bootstrap test (1000 replicates) is shown next to the branches. The evolutionary distances were computed using the Poisson correction method and are in the units of the number of amino acid substitutions per site (Adapted from Venegas-Calerón et al. [30]).

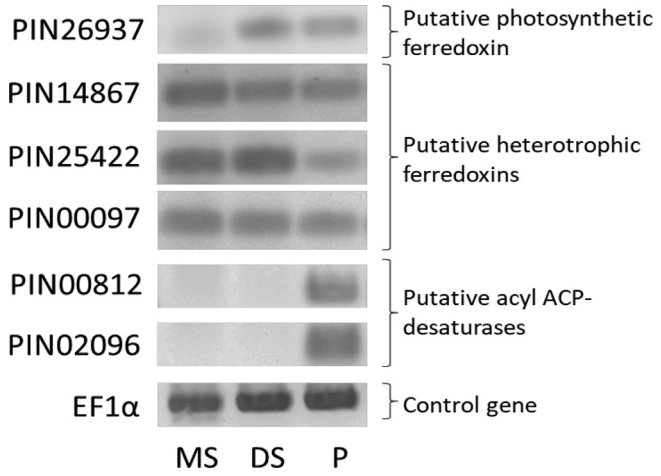

Fig. 5. Expression analysis of genes of interest. The expression of genes encoding ferredoxins and desaturases of interest was studied in mature seeds (MS), developing seeds (DS), and pods (P).

Table 5
Percentage of fatty acids detected in *H. impetiginosus* seed oil.

Common name	Systematic name	FAME	%*
Palmitic acid	Hexadecanoic acid	C16:0	10.4
Palmitoleic acid	(9Z)-Hexadec-9-enoic acid	C16:1Δ^{9}	6
Margaric acid	Heptadecanoic acid	C17:0	0.9
Stearic acid	Octadecanoic acid	C18:0	8.9
Oleic acid	(9Z)-Octadec-9-enoic acid	C18:1Δ^{9}	45.9
Linoleic acid	(9Z,12Z)-octadeca-9,12-dienoic acid	C18:2$\Delta^{9,12}$	22.1
Arachidic acid	Eicosanoic acid	C20:0	3.7
Gondoic acid	(11Z)-Eicos-11-enoic acid	C20:1Δ^{11}	1.2
Other			0.8
Total Saturated			23.9
Total Monounsaturated			53.1
Total Polyunsaturated			22.1

* represents the percentage of the total peak area.

palmitoleic acid synthesis activity as suggested by Schultz et al. [18].

A GC–MS analysis of the fatty acid profile of seed oil of *H. impetiginosus* showed an accumulation of up to 6% of palmitoleic acid (Table 5). While it can be considered as a modest accumulation, it is still significantly higher than the percentage of accumulation of palmitoleic acid in the average plant seed oil. The putative palmitoyl-ACP desaturases expression in the pod and not in the developing or mature seeds might account in part for that relatively low accumulation of palmitoleic acid in seed oil. While these results confirm the validity of our bioinformatic approach, it also confirms that the palmitoleic acid accumulation phenotype is multifactorial. It is noteworthy that the palmitic acid percentage (10.4%) is higher than that of palmitoleic acid (6%). This suggests that the availability of the substrate (palmitic acid) may not be the limiting factor. To succeed in identifying plant species with a higher proportion of palmitoleic acid in seed oil, the bioinformatic approach needs to be tweaked to consider additional factors implicated in this process. This highlights the need for further research to fully understand the molecular and biochemical bases of palmitoleic acid accumulation in seed oil. Gene expression localization is as important as the catalytic activity of the enzymes of interest in determining unusual fatty acid accumulation in seed oil. One possible improvement on the proposed bioinformatics approach is to integrate promoter analysis studies that look for the presence of seed-specific motives. That would suggest a gene expression localization in seeds, increasing the likelihood of accumulation of palmitoleic acids in seed oil.

5. Conclusions

The bioinformatic approach that consists in identifying acyl-ACP desaturase sequences that contain an F, Y, or W amino acid in position 151 proved to be useful to identify a plant species that accumulates palmitoleic acid in its seed oil. The presence of phenylalanine in position 151 of the desaturase seems to have a similar structural role to that of tryptophan. However, the low accumulation percentage of the observed palmitoleic acid (6%) indicate that: i) the presence of a divergent desaturase with the right variations is necessary but not enough for the accumulation of palmitoleic acid in seed oil and ii) the bioinformatic approach proposed in this study needs to integrate other factors that are important for palmitoleic acid accumulation to be useful for the identification of plant species that accumulate high levels of this unusual fatty acid, such as the identification of seed specific motives in the promoter of the desaturases of interest.

Author contributions

- Study conception and design: EG El-Kassis; ZN Juárez
- Data collection: G Salazar-Robles; LR Hernández; M Rodríguez-Acosta; Y Pedraza-Pérez; E Bautista-Rodríguez
- Analysis and interpretation of results: G Salazar-Robles; EG El-Kassis; M Rodríguez-Acosta; Y Pedraza-Pérez; LR Hernández; ZN Juárez
- Draft manuscript preparation: G Salazar-Robles; EG El-Kassis
- Revision of the results and approved the final version of the manuscript: EG El-Kassis; ZN Juárez; B Pérez-Armendáriz

Financial support

This work has been supported by a scholarship grant from the Consejo Nacional de Ciencia y Tecnología (CONACYT) to G.S.R. and a grant from the Research Department of the Universidad Popular Autónoma del Estado de Puebla to E.G.E.,

Conflict of interest

None.

Acknowledgments

The authors would like to acknowledge Manuel Morales for technical assistance in localizing a *H. impetiginosus* tree.

Supplementary material

https://doi.org/10.1016/j.ejbt.2022.09.008.

References

[1] Wu Y, Li R, Hildebrand DF. Biosynthesis and metabolic engineering of palmitoleate production, an important contributor to human health and sustainable industry. Prog Lipid Res 2012;51(4):340–9. https://doi.org/10.1016/j.plipres.2012.05.001. PMid: 22658963.

[2] Fatima T, Snyder CL, Schroeder WR, et al. Fatty acid composition of developing sea buckthorn (*Hippophae rhamnoides* L.) berry and the transcriptome of the mature seed. PLoS One 2012;7(4):e34099. PMid: 22558083.

[3] Vinita PD, Kumari N. Potential health benefits of Sea buckthorn oil- A review. Agric Rev 2017;38(3):233–7. , https://doi.org/10.18805/AG.V38I03.8984.

[4] Hu W, Fitzgerald M, Topp B, et al. A review of biological functions, health benefits, and possible de novo biosynthetic pathway of palmitoleic acid in macadamia nuts. J Funct Foods 2019;62:103520. https://doi.org/10.1016/j.jff.2019.103520.

[5] Wang F, Gao B, Huang L, et al. Evaluation of oleaginous eustigmatophycean microalgae as potential biorefinery feedstock for the production of palmitoleic acid and biodiesel. Bioresour Technol 2018;270:30–7. https://doi.org/10.1016/j.biortech.2018.09.016. PMid: 30212771.

[6] Knothe G. Biodiesel derived from a model oil enriched in palmitoleic acid, macadamia nut oil. Energy Fuels 2010;24(3):2098–103. https://doi.org/10.1021/ef9013295.

[7] Cao Y, Liu W, Xu X, et al. Production of free monounsaturated fatty acids by metabolically engineered *Escherichia coli*. Biotechnol Biofuels 2014;7:59. https://doi.org/10.1186/1754-6834-7-59. PMid: 24716602.

[8] Sun X, Duan A, Gao G, et al. Optimization of *Decaisnea insignis* seed oil extraction process and analysis of fatty acid. Sci Technol Food Ind 2012;33:236–41.

[9] Jedidi B, Mokbli S, Sbihi HM, et al. Effect of extraction solvents on fatty acid composition and physicochemical properties of *Tecoma stans* seed oils. J King Saud Univ - Sci 2020;32(4):2468–73. https://doi.org/10.1016/j.jksus.2020.03.044.

[10] Aquino-Bolaños EN, Mapel-Velazco L, Martín-del-Campo ST, et al. Fatty acids profile of oil from nine varieties of *Macadamia nut*. Int J Food Prop 2017;20(6):1262–9. https://doi.org/10.1080/10942912.2016.1206125.

[11] Tupec M, Culka M, Machara A, et al. Understanding desaturation/hydroxylation activity of castor stearoyl Δ^9-Desaturase through rational mutagenesis. Comput Struct Biotechnol J 2022;20:1378–88. https://doi.org/10.1016/j.csbj.2022.03.010. PMid: 35386101.

[12] Cahoon EB, Lindqvist Y, Schneider G, et al. Redesign of soluble fatty acid desaturases from plants for altered substrate specificity and double bond position. Proc Natl Acad Sci 1997;94(10):4872–7. https://doi.org/10.1073/pnas.94.10.4872. PMid: 9144157.

[13] Troncoso-Ponce MA, Barthole G, Tremblais G, et al. Transcriptional activation of two delta-9 palmitoyl-ACP desaturase genes by MYB115 and MYB118 is critical for biosynthesis of omega-7 monounsaturated fatty acids in the endosperm of Arabidopsis seeds. Plant Cell 2016;28(10):2666–82. https://doi.org/10.1105/tpc.16.00612. PMid: 27681170.

[14] Cahoon EB, Shah S, Shanklin J, et al. A determinant of substrate specificity predicted from the acyl-acyl carrier protein desaturase of developing cat's claw seed. Plant Physiol 1998;117(2):593–8. https://doi.org/10.1104/pp.117.2.593. PMid: 9625712.

[15] Cahoon EB, Shanklin J. Substrate-dependent mutant complementation to select fatty acid desaturase variants for metabolic engineering of plant seed oils. Proc Natl Acad Sci 2000;97(22):12350–5. https://doi.org/10.1073/pnas.210276297. PMid: 11027301.

[16] Liu B, Sun Y, Xue J, et al. Stearoyl-ACP Δ^9 desaturase 6 and 8 (GhA-SAD6 and GhD-SAD8) are responsible for biosynthesis of palmitoleic acid specifically in developing endosperm of upland cotton seeds. Front Plant Sci 2019;10:703. https://doi.org/10.3389/fpls.2019.00703. PMid: 31214221.

[17] Moreno-Pérez AJ, Sánchez-García A, Salas JJ, et al. Acyl-ACP thioesterases from macadamia (*Macadamia tetraphylla*) nuts: Cloning, characterization and their impact on oil composition. Plant Physiol Biochem 2011;49(1):82–7. https://doi.org/10.1016/j.plaphy.2010.10.002. PMid: 21071236.

[18] Schultz DJ, Suh MC, Ohlrogge JB. Stearoyl-acyl carrier protein and unusual acyl-acyl carrier protein desaturase activities are differentially influenced by ferredoxin. Plant Physiol 2000;124(2):681–92. https://doi.org/10.1104/pp.124.2.681. PMid: 11027717.

[19] Kazaz S, Miray R, Baud S. Acyl-Acyl carrier protein desaturases and plant biotic interactions. Cells 2021;10(3):674. https://doi.org/10.3390/cells10030674. PMid: 33803674.

[20] Salk JJ, Schmitt MW, Loeb LA. Enhancing the accuracy of next-generation sequencing for detecting rare and subclonal mutations. Nat Rev Genet 2018;19:269–85. https://doi.org/10.1038/nrg.2017.117. PMid: 29576615.

[21] Ma X, Shao Y, Tian L, et al. Analysis of error profiles in deep next-generation sequencing data. Genome Biol 2019;20:50. https://doi.org/10.1186/s13059-019-1659-6. PMid: 30867008.

[22] Waterhouse A, Bertoni M, Bienert S, et al. SWISS-MODEL: homology modelling of protein structures and complexes. Nucleic Acids Res 2018;46(W1):W296–303. https://doi.org/10.1093/nar/gky427. PMid: 29788355.

[23] Bienert S, Waterhouse A, De Beer TAP, et al. The SWISS-MODEL Repository-new features and functionality. Nucleic Acids Res 2017;45(D1):D313–9. https://doi.org/10.1093/nar/gkw1132. PMid: 27899672.

[24] Studer G, Rempfer C, Waterhouse AM, et al. QMEANDisCo—distance constraints applied on model quality estimation. Bioinformatics 2020;36(6):1765–71. https://doi.org/10.1093/bioinformatics/btz828. PMid: 31697312.

[25] Bertoni M, Kiefer F, Biasini M, et al. Modeling protein quaternary structure of homo- and hetero-oligomers beyond binary interactions by homology. Sci Rep 2017;7:10480. https://doi.org/10.1038/s41598-017-09654-8. PMid: 28874689.

[26] Hanwell MD, Curtis DE, Lonie DC, et al. Avogadro: An advanced semantic chemical editor, visualization, and analysis platform. J Cheminform 2012;4:17. https://doi.org/10.1186/1758-2946-4-17. PMid: 22889332.

[27] Huang CC, Meng EC, Morris JH, et al. Enhancing UCSF Chimera through web services. Nucleic Acids Res 2014;42(W1):W478–84. https://doi.org/10.1093/nar/gku377. PMid: 24861624.

[28] Madeira F, Park YM, Lee J, et al. The EMBL-EBI search and sequence analysis tools APIs in 2019. Nucleic Acids Res 2019;47(W1):W636–41. https://doi.org/10.1093/nar/gkz268. PMid: 30976793.

[29] Chi X, Yang Q, Lu Y, et al. Genome-wide analysis of fatty acid desaturases in soybean (*Glycine max*). Plant Mol Biol Report 2011;29:769–83. https://doi.org/10.1007/s11105-010-0284-z.

[30] Venegas-Calerón M, Zambelli A, Ruiz-López N, et al. cDNA cloning, expression levels and gene mapping of photosynthetic and non-photosynthetic ferredoxin genes in sunflower (*Helianthus annuus* L.). Theor Appl Genet 2009;118:891–901. https://doi.org/10.1007/s00122-008-0947-4. PMid: 19130032.
[31] Ichihara K, Fukubayashi Y. Preparation of fatty acid methyl esters for gas-liquid chromatography. J Lipid Res 2010;51(3):635–40. https://doi.org/10.1194/jlr.D001065. PMid: 19759389.
[32] Rodríguez MF, Sánchez-García A, Salas JJ, et al. Characterization of soluble acyl-ACP desaturases from *Camelina sativa*, *Macadamia tetraphylla* and *Dolichandra unguis-cati*. J Plant Physiol 2015;178:35–42. https://doi.org/10.1016/j.jplph.2015.01.013. PMid: 25765361.
[33] Hall BG. Building phylogenetic trees from molecular data with MEGA. Mol Biol Evol 2013;30(5):1229–35. https://doi.org/10.1093/molbev/mst012. PMid: 23486614.
[34] Nguyen HT, Park H, Koster KL, et al. Redirection of metabolic flux for high levels of omega-7 monounsaturated fatty acid accumulation in camelina seeds. Plant Biotechnol J 2015;13(1):38–50. https://doi.org/10.1111/pbi.12233. PMid: 25065607.
[35] Silva-Junior OB, Grattapaglia D, Novaes E, et al. Genome assembly of the Pink Ipê (*Handroanthus impetiginosus*, *Bignoniaceae*), a highly valued, ecologically keystone Neotropical timber forest tree. GigaScience 2018;7(1):gix125. https://doi.org/10.1093/gigascience/gix125. PMid: 29253216.
[36] Lou Y, Schwender J, Shanklin J. FAD2 and FAD3 desaturases form heterodimers that facilitate metabolic channeling *in vivo*. J Biol Chem 2014;289(26):17996–8007. https://doi.org/10.1074/jbc.M114.572883. PMid: 24811169.
[37] Ettaki H, Troncoso-Ponce MA, To A, et al. Overexpression of *MYB115, AAD2*, or *AAD3* in *Arabidopsis thaliana* seeds yields contrasting omega-7 contents. PLoS ONE 2018;13(1):e0192156. https://doi.org/10.1371/journal.pone.0192156. PMid: 29381741.
[38] Kazaz S, Miray R, Lepiniec L, et al. Plant monounsaturated fatty acids: Diversity, biosynthesis, functions and uses. Prog Lipid Res 2022;85:101138. https://doi.org/10.1016/j.plipres.2021.101138. PMid: 34774919.
[39] Bennet EJ, Roberts JA, Wagstaff C. The role of the pod in seed development: strategies for manipulating yield. New Phytol 2011;190(4):838–53. https://doi.org/10.1111/j.1469-8137.2011.03714.x. PMid: 21507003.
[40] Zhang W, Mao P, Li Y, et al. Assessing of the contributions of pod photosynthesis to carbon acquisition of seed in alfalfa (*Medicago sativa* L.). Sci Rep 2017;7:42026. https://doi.org/10.1038/srep42026. PMid: 28169330.